Commun. Theor. Phys. (Beijing, China) **52** (2009) pp. 701–706

Vol. 52, No. 4, October 15, 2009

First-Principles Study of Structural, Elastic and Electronic Properties of OsSi*

LI Jin,[1,2,3] LINGHU Rong-Feng,[1,4] YANG Ze-Jin,[1] CAO Yang,[2,3] and YANG Xiang-Dong[1,†]

[1]Institute of Atomic and Molecular Physics of Sichuan University, Chengdu 610065, China

[2]College of Material and Chemical Engineering, Hainan University, Haikou 570228, China

[3]Hainan Provincial Key Laboratory of Research on Utilization of Si-Zr-Ti Resources, Haikou 570228, China

[4]School of Physics and Electronic Science, Guizhou Normal University, Guiyang 550001, China

(Received October 22, 2008; Revised February 25, 2009)

Abstract *First-principles study of structural, elastic, and electronic properties of the B20 structure OsSi has been reported using the plane-wave pseudopotential density functional theory method. The calculated equilibrium lattice and elastic constants are in good agreement with the experimental data and other theoretical results. The dependence of the elastic constants, the aggregate elastic modulus, the deviation from the Cauchy relation, the elastic wave velocities in different directions and the elastic anisotropy on pressure have been obtained and discussed. This could be the first quantitative theoretical prediction of the elastic properties under high pressure of OsSi compound. Moreover, the electronic structure calculations show that OsSi is a degenerate semiconductor with the gap value of 0.68 eV, which is higher than the experimental value of 0.26 eV. The analysis of the PDOS reveals that hybridization between Os d and Si p states indicates a certain covalency of the Os-Si bonds.*

PACS numbers: 62.20.D-, 71.20.Nr, 71.15.Mb
Key words: OsSi, elastic constants, electronic properties, high pressure effect

1 Introduction

Semiconducting transition metal silicides are a very important class of semiconductors, which are considered to be promising for photoelectronic and thermoelectric applications. As one of the narrow band gap semiconducting monsilicides, OsSi has attracted considerable attention due to its practical importance in new silicon-compatible devices.[1] Therefore, the knowledge of its elastic and electronic properies is very useful from the point of view of device application.

Powder diffraction experiment[2] showed that OsSi forms in a peritectic reaction at 1730 °C, just below the liquidus curve of the system. In addition the thermoelectric and magnetic properties of OsSi both below and above room temperature has been investigated. Liu *et al.*[3] found the phase diagrams and thermodynamic properties of the Os-Si system using the CALPHAD technique. Bond distance, vibrational frequency, electron affinity, ionization potential, dissociation energy, and dipole moment of OsSi molecule in neutral, positively, and negatively charged ion were studied using the density functional method by Wu *et al.*[4] Minisini *et al.*[5] reported elastic and thermodynamic properties of OsSi by the VASP code with the projected augmented wave method as implemented in the MedeA interface. The electronic band structure of OsSi was mainly discussed in other literatures.[6−9]

The main goal of this work is shedding light on the ground structure of OsSi and giving a detailed description for the structural and elastic properties of this compound at different pressures by using first-principles calculations. The band-structural character, total and projected density of states are also investigated. The calculated results are compared with the available experimental data and the previous works. The method of calculation is given in Sec. 2. The results and overall conclusion are presented and discussed in Sec. 3.

2 Theoretical Methods

2.1 *Ab Initio Method*

Our calculations have been made using the plane-wave pseudopotential density functional theory method, as invoked by the Cambridge serial total energy package (CASTEP) program.[10−11] The major advantages of this approach are: the ease of computing forces and stresses; good convergence control with respect to all computational parameters employed; favourable scaling with number of atoms in the system and the ability to make cheaper calculations by neglecting core electrons.[12] The effects of exchange–correlation interaction are treated with the gen-

*Supported by the National Natural Science Foundation of China under Grant No. 10974139, the Doctoral Program Foundation of Institution of Higher Education of China under Grant No. 20050610010, the Natural Science Foundation of the Education Bureau of Guizhou Province of China under Grant No. 2005105 and the Governor's Foundation for Science and Education Elites of Guizhou Province under Grant No. QSZHZ2006(113)

†Corresponding author, E-mail: xdyang@scu.edu.cn

eralized gradient approximation (GGA) of Perdew–Wang (1991) version (PW91)[13−14] and the local density approximation (LDA) of Ceperley and Alder.[15] The electronic wave functions are expanded in a plane wave basis set with energy cut-off of 400 eV. Valence electrons are Os $5s^25p^65d^66s^2$ and Si $3s^23p^2$. For the Brillouin-zone sampling, we use the Monkhorst–Pack mesh with $8 \times 8 \times 8$ k-points, where the self-consistent convergence of the total energy is at 10^{-6} eV/atom. These parameters are sufficient in leading to well converged total energy, geometrical configurations, and elastic stiffness coefficients. All the total energy electronic structure calculations are implemented with the non-local ultrasoft pseudopotential introduced by Vanderbilt.[16]

2.2 *Elastic Properties*

The elastic constants of solids provide a link between the mechanical and dynamical behaviours of crystals, and give important information concerning the nature of the forces operating in solids. The elastic constants are defined by means of a Taylor expansion of the total energy, $E(V, \delta)$, of the system with respect to a small strain δ of the lattice volume V. We can express the energy of a strained system as follows:[17]

$$E(V,\delta) = E(V_0,0) + V_0\Big[\sum_i \tau_i\xi_i\delta_i + \frac{1}{2}\sum_{ij} c_{ij}\delta_i\xi_j\delta_j\Big]\,, \quad (1)$$

where $E(V_0,0)$ is the energy of the unstrained system with volume V_0; τ_i is an element in the stress tensor, ζ_i is a factor to take care of Voigt index. Since the stress and strain tensors are symmetric, the most general elastic stiffness tensor has only 21 non-zero independent components. For a cubic crystal, they are reduced to three components, i.e. c_{11}, c_{12}, and c_{44}. All these elastic constants can be determined by computing the stress generated by forcing a small strain to an optimized unit cell.[18−19]

Moreover, we have calculated the main elastic parameters for cubic OsSi, namely, bulk modulus (B), shear modulus (G), and Young modulus (Y). These elastic parameters are usually calculated by two approximations: due to Voigt (V)[20] and Reuss (R),[21] in the following forms

Bulk modulus:

$$B_{V,R} = (c_{11} + 2c_{12})/3\,, \quad (2)$$

Shear modulus:

$$G_V = (c_{11} - c_{12} + 3c_{44})/5\,, \quad (3)$$

$$G_R = 5(c_{11} - c_{12})c_{44}/[4c_{44} + 3(c_{11} - c_{12})]\,, \quad (4)$$

we have utilized the VRH approximation[20−22] to evaluate the corresponding parameters of the polycrystalline species. In this approach, according to Hill, the Voigt and Reuss averages are limits and the actual effective moduli for polycrystals could be approximated by the arithmetic mean of these two bounds. From the values of $B_{\rm VRH}$ and $G_{\rm VRH}$ by the VRH approach, the Young modulus (Y) for polycrystalline OsSi was obtained as

$$Y_{\rm VRH} = \frac{9B_{\rm VRH}}{1 + 3B_{\rm VRH}/G_{\rm VRH}}\,. \quad (5)$$

3 Results and Discussion

Within ab initio calculations, the structural properties are very important first step to understand the material properties from a microscopic point of view. The compound OsSi crystallizes in the FeSi-type cubic B20 structure.[23] This structure has 12 symmetry operations. The space group is $P2_13$ (198) and the point symmetry at the osmium or silicon site is $C3$.

Table 1 Lattice parameter a, bulk modulus B_0, its pressure derivative B_0', and elastic constant parameters together with the experimental data and other theoretical results for the B20 structure OsSi at 0 GPa and 0 K.

Structural	Present work		Experiment		Other theoretical works		
propertices	GGA	LDA	[25]	[2]	GGA[5]	LDA[5]	GGA[6]
a (Å)	4.7874	4.7026	4.727	4.7305	4.79	4.73	4.829
B_0 (GPa)	215.9	250.7			211	238	265
B_0' (GPa)	5.0	4.9					
c_{11} (GPa)	280.4	296.8			245	274	
c_{12} (GPa)	173.9	202.4			194	220	
c_{44} (GPa)	156.3	169.8			150	161	

To obtain the ground state value of lattice parameter, the total energy E of the B20 structure OsSi has been calculated at different primitive cell volume, then a least-square fits of these energy-volume (E-V) data are made to the Brich–Murnaghan's equation of state (B-M EOS).[24] The obtained lattice constant a, the bulk modulus B_0, and its pressure derivative B_0', as well as the elastic constants at zero temperature and pressure are

presented in Table 1, together with the available experimental values[2,25] and other theoretical results.[5−6] The pressure dependence of the relative volume V/V_0 at 0 K is illustrated in Fig. 1. It is demonstrated that out calculated results are in satisfactory agreement with the experimental data[2,25] and other theoretical results.[5−6] As expected the GGA method overestimates the lattice constant a and underestimate bulk modulus B_0. Notice that the experimental data of lattice constant is included between the LDA and GGA result.

We have also calculated the pressure dependence of the internal coordinate parameters of silicon and osmium atom with GGA level. The calculated values are plotted in Fig. 1. It is shown that, as the pressure increases, the fractional coordinates of silicon and osmium atoms increase monotonically, the interatomic distance decrease monotonically and their interactions become stronger.

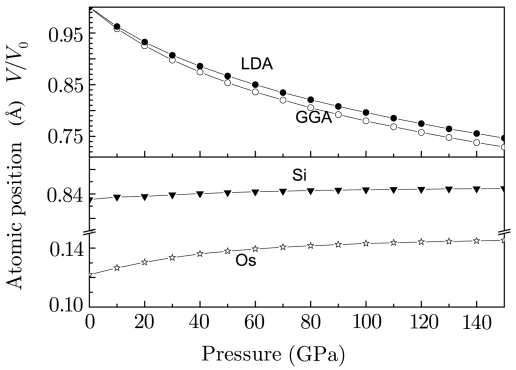

Fig. 1 The pressure dependence of the relative volume V/V_0 of OsSi and the fractional coordinates of silicon, osmium atoms.

Table 2 The elastic constants (GPa) and the aggregate elastic modulus (GPa) calculated within the GGA for the B20 structure OsSi at zero temperature and different pressures (GPa).

P	c_{11}	c_{12}	c_{44}	B	G	Y
0	280.4	173.9	156.3	209.4	101.5	262.3
10	332.5	220.8	165.0	258.1	106.9	281.9
20	377.9	262.3	171.3	300.8	110.9	296.4
30	438.5	311.1	183.0	353.6	120.0	323.4
40	516.6	345.8	190.5	402.7	138.0	371.7
50	585.7	381.0	200.9	449.3	153.3	412.9
60	665.1	411.7	208.5	496.2	170.7	459.6
70	728.8	442.3	216.8	537.8	183.6	494.6
80	794.5	472.7	224.7	580.0	196.5	529.8
90	855.6	501.4	233.6	619.5	209.1	563.8
100	912.4	530.8	242.3	658.0	220.2	594.3
110	969.4	561.5	252.4	697.5	231.7	626.0
120	1024.5	587.1	258.2	732.9	241.6	653.0
130	1077.6	613.8	265.1	768.4	251.2	679.7
140	1129.1	641.2	272.8	803.8	260.9	706.3
150	1183.4	668.3	277.8	840.0	269.5	730.5

In Table 2, we have presented the pressure dependence of the elastic constants c_{ij} and the aggregate elastic modulus (B, G, and Y) calculated within the GGA for the B20 structure OsSi at zero temperature and different pressures. Although there are no available values to compare with out calculated results, our data will be beneficial to future investigation. One condition for mechanical stability of a structure is that its strain energy must be positive against any homogeneous elastic deformation. For cubic crystals, this imposes the following constraints:[26]

$$C_{44} > 0, \quad C_{11} > |C_{12}|, \quad C_{11} + 2C_{12} > 0\,, \qquad (6)$$

where $C_{\alpha\alpha} = c_{\alpha\alpha} - P$ ($\alpha = 1, 4$), $C_{12} = c_{12} + P$. It is obvious from Table 2 that the elastic constants under applied pressure are content with Eq. (6), indicating that this compound is stable against elastic deformation.

The relation of pressure with elastic constants for OsSi is plotted in Fig. 2. The dependence of bulk modulus, the shear modulus, and Young modulus on pressure are shown in Fig. 3. It has been found that c_{11} varies substantially under the pressure when compared with the variations in c_{12} and c_{44}. The elastic constant c_{11} represents elasticity in length. A longitudinal strain produces a change in c_{11}. The elastic constants c_{12} and c_{44} are related to the elasticity in shape, which is a shear constant. A transverse strain causes a change in shape without a change in volume. Therefore, c_{12} and c_{44} are less sensitive of pressure as compared with c_{11}. As pressure increase, the elastic constants and the aggregate elastic modulus for the B20 structure OsSi at zero temperature increase monotonically.

We might study theoretically the elasticity of OsSi by means of models which assume that the interatomic forces have a certain shape and directionality. One common approaches is to assume that the atoms are connected with springs and that the resulting forces are only in the direc-

tion of the nearest neighbors (central force mode). The deviation from the Cauchy relation $\delta = c_{12} - c_{44} - 2P$ is a measure of the contribution from the noncentral many-body force since the Cauchy relation $c_{12} = c_{44} + 2P$ should be satisfied when interatomic potentials are purely central. Figure 4 shows the pressure dependence of δ. The deviation δ becomes larger as the pressure increases, which proved that the noncentral many-body force becomes more and more important at high pressure. Thus, it is necessary to consider third-order and fourth-order elastic constants when the anharmonic properties of OsSi are discussed by means of elastic constants at high pressure.

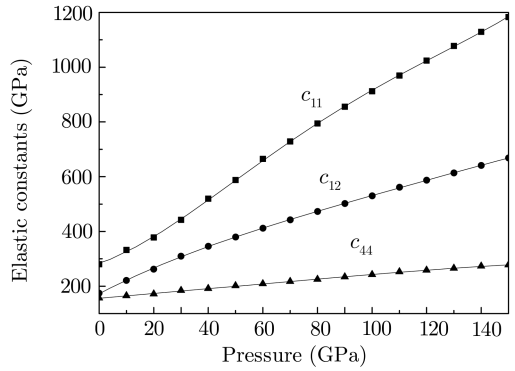

Fig. 2 Static elastic constants of OsSi as a function of pressure.

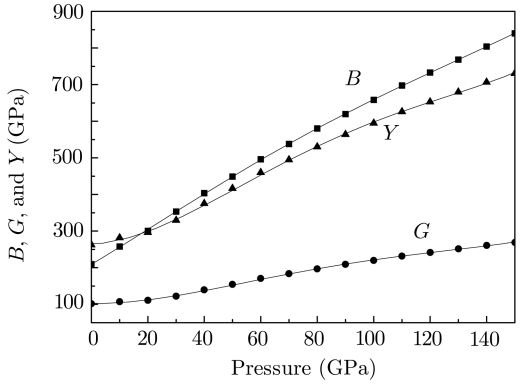

Fig. 3 Elastic modulic of OsSi as a function of pressure.

From the theoretical elastic constants, we computed the elastic wave velocities in different directions. The elastic wave velocities in different directions are given by[27−28]

$$V_i(\hat{g}) = \sqrt{C_i(\hat{g})/\rho}\,, \tag{7}$$

where i indicates the polarization and $\hat{g}$ the propagation direction of the wave, ρ is the mass density, and $C_i(\hat{g})$ is an appropriate combination of elastic constants, given by

$$\begin{aligned}
&C_{[100]}([100]) = c_{11} = V_{P1}^2\rho\,,\\
&C_{[110]}([110]) = \frac{1}{2}(c_{11}+c_{12}+2c_{44}) = V_{P2}^2\rho\,,\\
&C_{[111]}([111]) = \frac{1}{3}(c_{11}+2c_{12}+4c_{44}) = V_{P3}^2\rho\,,\\
&C_{[010]}([100]) = C_{[001]}([100]) = C_{[001]}([110]) = c_{44}\\
&\qquad = V_{S1}^2\rho\,,\\
&C_{[1\bar{1}0]}([110]) = \frac{1}{2}(c_{11}-c_{12}) = V_{S2}^2\rho\,,\\
&C_{[1\bar{1}0]}([111]) = C_{[11\bar{2}]}([111]) = \frac{1}{3}(c_{11}-c_{12}+c_{44})\\
&\qquad = V_{S3}^2\rho\,,
\end{aligned} \tag{8}$$

where V_p is the longitudinal wave with polarization parallel to the direction of propagation and V_s is the shear waves with polarization perpendicular to the direction of propagation. Figure 5 shows the pressure dependence of the elastic wave velocities along [100], [110], and [111] directions for OsSi. It is seen that all of the elastic wave velocities increase with increasing pressure. Obviously, longitudinal waves are fastest propagated along [111] and shear waves are slowest propagated along [110] and polarized along $[1\bar{1}0]$ at high pressure.

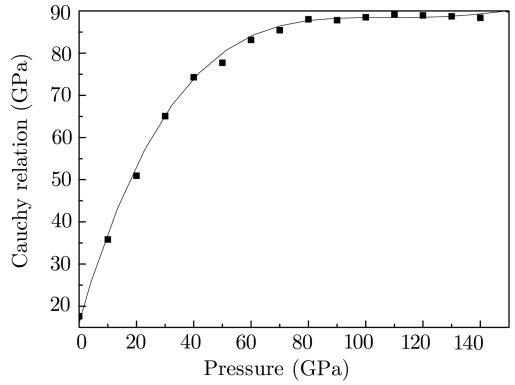

Fig. 4 The pressure dependence of the Cauchy relation of OsSi.

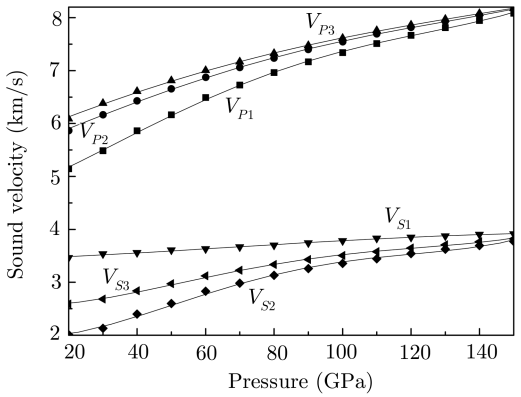

Fig. 5 The elastic wave velocities in different directions versus pressure for OsSi.

The elastic anisotropy of crystals has an important implication for engineering science since it is highly correlated with the possibility to induce microcracks in the materials.[29] The anisotropy factor for cubic crystals, $A = (2c_{44}+c_{12})/c_{11}$, has therefore been evaluated to provide insight on the elastic anisotropy of the B20 structure OsSi. For a completely isotropic material the A factor takes the value of 1, while values smaller or greater than unity measure the degree of elastic anisotropy.[30] Figure 6

shows the pressure dependence of the elastic anisotropy A of OsSi. We can find that the B20 structure OsSi exhibits large elastic anisotropy at zero pressure and the degree of the anisotropy decreases with pressure. When the applied pressures are larger than 100 GPa, the elastic anisotropy A nearly approaches to the value of 1. It means that OsSi is most elastically isotropic material at higher pressure.

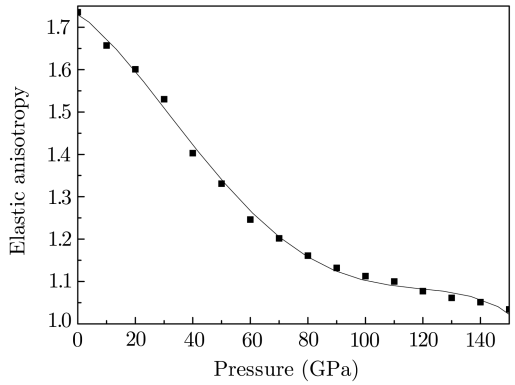

Fig. 6 The pressure dependence of the elastic anisotropy of OsSi.

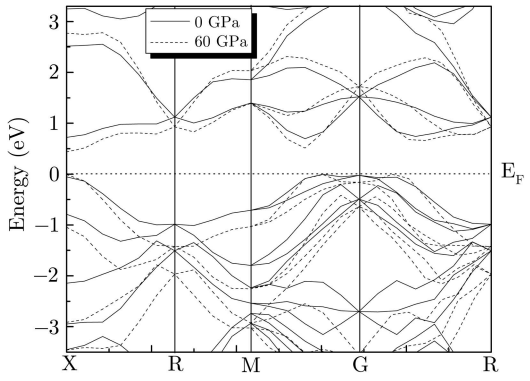

Fig. 7 Band structures of OsSi obtained using the GGA scheme calculated along high-symmetry directions in the Brillouin zone at 0 GPa and 60 GPa.

Figure 7 shows the band structure near the main Kohn–Sham band gap of OsSi at 0 GPa and 60 GPa according to the GGA calculation. The zero of energy is chosen to coincide with the top of the valence band. OsSi behaves as a degenerate semiconductor as can be inferred from its band diagram. In the absence of applied pressure the band structure of OsSi is characterized by an indirect transition of 0.68 eV between the valence band maximum and the conduction band minimum situated along the M-G direction (approximately at $0.7\times$ M-G and at $0.5\times$M-G, respectively). Our calculated result is in good agreement with previous first-principles computations.[6,8] However, the band gap overestimates the experimental value of 0.26 eV,[31] due to the strong component of metal d states near the gap.[6]

From the band structure, we can remark that when pressure increases, the valence bands and conduction bands for OsSi become dispersive, which imply that the interaction between Os and Si are more covalent. This leads to the decrease in the indirect band gap of OsSi under pressure. The pressure dependence of the energy band gap is shown in Fig. 8.

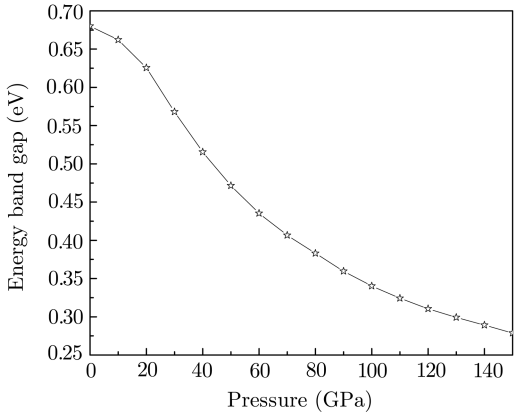

Fig. 8 Energy band gap as a function with the applied pressures.

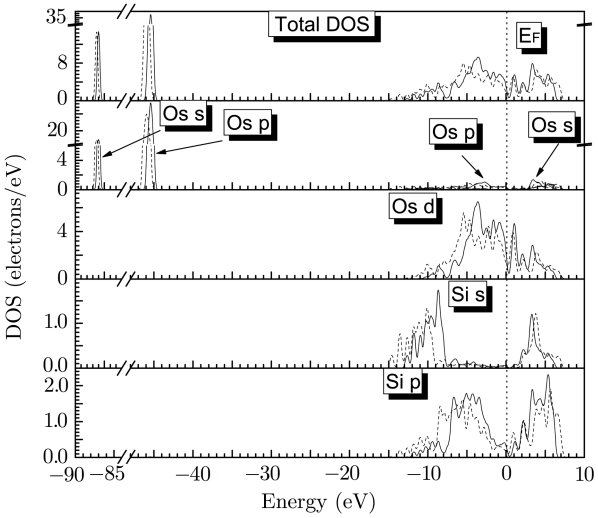

Fig. 9 Calculated total and projected density of states for OsSi at 0 GPa and 60 GPa with GGA level. The solid and dashed lines correspondence to 0 GPa and 60 GPa, respectively. The dotted vertical line refers to the Fermi level.

To further elucidate the nature of the electronic band structure, we have also calculated the total (DOS) and atomic site projected (PDOS) densities of states of this compound under $P = 0$ GPa, together with $P = 60$ GPa. These are displayed in Fig. 9. From the PDOS we are able to identify the angular momentum character of the different structures. Following Fig. 9, we should emphasis that there are five distinct structures in the density of electronic states separated from each other by gaps. In the absence of applied pressure the lowest valence bands situated in the range -86.07 to -86.04 eV are due to the Os s states. The structure localized between -45.7 and -45.3 eV is resulting from Os p orbital. The structure situated in the range -13.09 to -8.02 eV is essentially dominated by Si s states, with admixture from Os d and Si p states. The upper valence bands (between -7.57 and

0 eV) below the Fermi level are mainly due to Os d states hybridized with some Si p electrons, which indicates a certain covalency of the Os-Si bonds. The conduction bands localized between 0 and 6.32 eV above the Fermi lever are mainly Os d states hybridized with some Si p and s electrons giving rise to antibonding bands.

From Fig. 9 we can see that when pressure increases, the peaks of Os d, Si p, and Si s states decrease, but the bandwidth becomes broad, which implies that the electrons in those states are active under pressure. The change of PDOS can be attributed to charge transfer during lattice distortion. With the increasing of pressures, higher overlap of Os d and Si p states (concluding little Si s states) results in a stronger delocalization of electrons. Electrons will transfer from the majority to minority spin band and form broader bands. It is evidently indicative of a covalent interaction between Os and Si atoms resulting from strong hybridization. This leads to higher potential hardness under pressure in this compound, as already established from the bulk modulus (see Fig. 3).

In summary, we have studied the structural, elastic, and electronic properties of the B20 structure OsSi by first-principles calculations in the framework of the density functional theory. Our theoretical study concludes the following features: (i) The calculated equilibrium structural parameter and elastic constants are in good agreement with the experimental data and other theoretical results; (ii) The elastic properties have been investigated. The dependence of the elastic constants, the aggregate elastic modulus, the deviation from the Cauchy relation, the elastic wave velocities in different directions, and the elastic anisotropy on pressure have been obtained and discussed. To the best of our knowledge, there are no earlier studies on the effect of pressure on the elastic properties, we feel that our calculations can be use to cover the lack of data of this compound; (iii) The electronic structure calculations show that OsSi is a degenerate semiconductor with the gap value of 0.68 eV. The band gap is higher than the experimental value of 0.26 eV, due to the strong component of metal d states near the gap. The analysis of the PDOS also reveals that hybridization between Os d and Si p states indicates a certain covalency of the Os-Si bonds, which contributes to the hardness and fundamental properties.

References

[1] V.E. Borisenko (Ed.), *Semiconducting Silicides*, Springer, Berlin (2000).

[2] H. Hohl, A.P. Ramirez, C. Goldmann, G. Ernst, and E. Bucher, J. Alloys Comp. **278** (1998) 39.

[3] Y.Q. Liu, G. Shao, and K.P. Homewood, J. Alloys Comp. **320** (2001) 72.

[4] Z.J. Wu and Z.M. Su, J. Chem. Phys. **124** (2006) 184306.

[5] B. Minisini, J. Roetting, and F. Tsobnang, Comput. Mater. Sci. **43** (2008) 812.

[6] G.M. He, S.P. Li, and M.C. Huang, Chin. Phys. Lett. **18** (2001) 1389.

[7] Y. Imai, M. Mukaida, K. Kobayashi, and T. Tsunoda, Intermetallics **9** (2001) 261.

[8] Y. Imai and A. Watanabe, J. Alloys Comp. **417** (2006) 173.

[9] Y. Imai and A. Watanabe, Intermetallics **16** (2008) 769.

[10] M.C. Payne, M.P. Teter, D.C. Allan, T.A. Arias, and J.D. Joannopoulos, Rev. Mod. Phys. **64** (1992) 1045.

[11] V. Milman, B. Winkler, J.A. White, C.J. Packard, M.C. Payne, E.V. Akhmatskaya, and R.H. Nobes, Int. J. Quantum Chem. **77** (2000) 895.

[12] A. Bouhemadou, R. Khenata, M. Kharoubi, and Y. Medkour, Solid State Commun. **146** (2008) 175.

[13] J.P. Perdew, K. Burke, and M. Ernzerhof, Phys. Rev. Lett. **77** (1996) 3865.

[14] B. Hammer, L.B. Hansen, and J.K. Norskov, Phys. Rev. B **59** (1999) 7413.

[15] D.M. Ceperly and B.J. Alder, Phys. Rev. Lett. **45** (1980) 566.

[16] D. Vanderbilt, Phys. Rev. B **41** (1990) 7892.

[17] L. Fast, J.M. Wills, B. Johansson, and O. Eriksson, Phys. Rev. B **51** (1995) 17431.

[18] B.B. Karki, L. Stixrude, S.J. Clark, M.C. Warren, G.J. Ackland, and J. Crain, Am. Miner. **82** (1997) 51.

[19] R.M. Wentzcovitch, N.L. Ross, and G.D. Price, Phys. Earth Planet. Inter. **90** (1995) 101.

[20] W. Voigt, *Lehrbuch der Kristallphysik*, Teubner, Leipzig (1928).

[21] A. Reuss and Z. Angew, Math. Mech. **9** (1929) 49.

[22] R. Hill, Proc. Phys. Soc. London A **65** (1952) 349.

[23] T.B. Massalski, *Binary Alloy Phase Diagrams*, (2nd ed.), ASM International, Ohio (1990).

[24] Y.D. Guo, X.L. Cheng, L.P. Zhou, Z.J. Liu, and X.D. Yang, Physica B **373** (2006) 33456.

[25] K. Göransson, I. Engström, and B. Noläng, J. Alloys. Comp. **219** (1995) 107.

[26] G.V. Sin'ko and N.A. Smirnow, J. Phys.: Condens. Matter **14** (2002) 6989.

[27] M. Prikhodko, M.S. Miao, and W.R.L. Lambrecht, Phys. Rev. B **66** (2002) 125201.

[28] W.F. Weston and A.V. Granato, Phys. Rev. B **12** (1975) 5355.

[29] V. Tvergaard and J.W. Hutchinson, J. Am. Ceram. Soc. **71** (1988) 157.

[30] M. Mattesini, R. Ahuja, and B. Johansson, Phys. Rev. B **68** (2003) 184108.

[31] B. Buschinger, W. Guth, M. Weiden, *et al.*, J. Alloys Compd. **262-263** (1997) 238.